

Color-Mixing Correction of Overlapped Colors in Scanner Images

Misako Suwa

IMAGE COMPUTING LABORATORY
FUJITSU LABORATORIES LTD.
Kawasaki-shi, Japan
e-mail: suwasan@labs.fujitsu.com

Abstract—Color mixing occurs between the colors of ink and paper when the former is non-opaque. For non-white paper, even the hue of a figure in such an ink may change. In such cases, color conversion is required to extract only the pattern of a specified ink-color from a document image. In this paper, we consider an effective model of the Yule-Nielsen type with the Beer-Lambert law for scanner images of handwritten forms with ballpoint pens, and propose a new method of correcting color mixing. These parameters are calculated using only the information obtained from a pair of scanner images with different-colored paper and the same ink color. The experimental results confirm the feasibility of this approach.

Keywords—component; OCR; scanner image; color-mixing correction; subtractive color-mixing; Yule-Nielsen equation

I. INTRODUCTION

Research on document image processing using color information has become active with the popularization of color scanners. One topic of interest is the extraction of postprints (stamps, handwritten characters, *etc.*) with ink of a specific color from a form image (*e.g.*, extraction of notes with a red ballpoint pen). With non-white paper and non-opaque ink, the problem becomes more difficult because of color mixing between the ink and paper. For example, the observed color of a figure with pink ink on blue paper tends to become purple rather than pink (see Fig. 1). In such cases, color-mixing correction is required to identify the true color.

It should be emphasized that the aim of this paper is not to make an exact model of color overlap as in [1]. Rather, it is to estimate an effective model that can be treated using only information obtained from scanner images, when neither the chemical data of the ink nor spectrophotometers are available. The simplest color-mixing models are linear models [2][3][4]. These models explain the color of a foreground figure as a linear combination of the fore- and background colors. In the case of a scanner image, another type of color-mixing—Gaussian-type blurring—occurs at the boundary of the figure because of the low-pass property of the optical system and the sampling process involved. Therefore, the color of a preprint is distributed along a line between the centers of the fore- and background colors [5]. This property is valid when the ink is opaque or its thickness is uniform. Attempts were made in [6][7] to separate overlapped pre- and postprints using this assumption. We introduced this property to extend the particle density model [4] to handle scanner images and proposed a method to correct color-mixing between the fore- and background

colors [8]. However, the approximation error increased when the ink had a chromatic color. This means that differences in the level of absorption among RGB channels caused by the uneven thickness of the ink are non-negligible.

This paper targets ballpoint pens as they are commonly used for handwritten forms. Here, the color distribution properties of a scanner image are first clarified. Subsequently, an effective model based on the $n=1$ Yule-Nielsen equation [9] with the Beer-Lambert law [10] is shown to approximate the distribution well. Using the model, we propose a color-mixing correction method that converts the color of postprints on any background color into that on white.

II. COLOR MIXING PROBLEM

Color-mixing occurs when colors overlap. If the background color is chromatic, even the hue of the foreground color may change. Fig. 1 shows an example of this effect. The distribution b corresponds to a postprint (foreground) with pink gel ink on pale blue paper (background) in RGB space. The distributions c and d correspond to postprints of purple and pink inks on white paper, respectively. The distribution b is much closer to c than to d. To extract the ‘pink’ pattern, b must be transformed to d. The average RGB values of each pattern are indicated below the images.



a. b,c,d in RGB space b. Pink on pale blue c. Purple on white d. Pink on white
Figure 1. Color-mixing of ink and paper

III. PROPERTIES OF SCANNER IMAGES

Before discussing the color-mixing model, we select a color coordinate system (CCS) and briefly explain the color distribution properties of a scanner image.

A. Selecting a Color Coordinate System

The $\gamma=1$ linear RGB (*l*RGB) is used for the color system in consideration of the following facts:

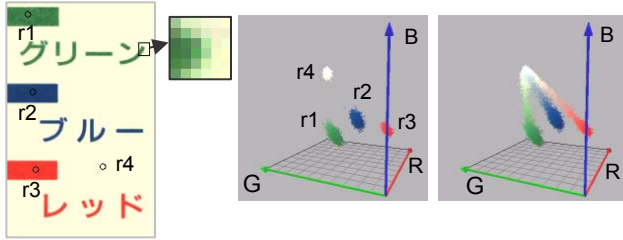
- The sensors of general document scanners observe RGB values independently.
- Nonlinear transformation of RGB elements makes it difficult to grasp the essence of the problem.

B. Color Distribution of a Scanner Image with Preprints

A scanned document image has characteristic qualities in its color distribution:

- The distribution of a single-color image becomes Gaussian because of the heat noise of the system.
- The distribution of a uniform color pattern becomes line-shaped because of the blurring at its boundary.

Examples of these cases are shown in Fig. 2. Fig. 2 a is a color form image with green, red, and blue preprints. The graph in the center corresponds to the distribution of regions far from the boundary indicated by the small circle, whereas the graph on the right corresponds to the distribution of the whole image. The colors of the latter distribute along three line segments originating from the average background color.

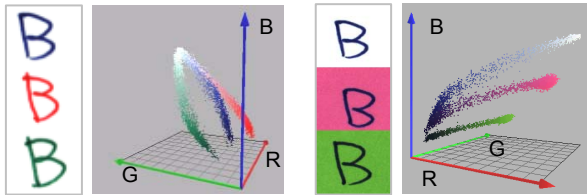


a. Color form image b. r1, r2, r3, r4 regions c. Whole image

Figure 2. Color distribution of a scanner image

C. Color Distribution of a Scanner Image with Postprints

In the case of postprints by a ballpoint pen, the color apparently distributes along a curve rather than a line segment. This could be due to the uneven thickness of the inks, as the absorption of light differs considerably at each point of the document depending on the thickness of the ink. Fig. 3 shows images that include handwritten characters of blue, red, and green inks and their color distributions. Each curve apparently starts from the center of the background color and ends at a dark point.



a. Blue, Red, and Green on White b. Blue on White, Pink, and Green

Figure 3. Color distribution of gel ink images

IV. MODEL SELECTION FOR MIXING

This section examines an effective model for color-mixing correction. The model should be able to explain color differences depending on the thickness of the ink.

A. Subtractive Mixture Model

The subtractive mixture model (SMM) with the Beer-Lambert law [10] is the simplest model that considers only

the absorption of light, therefore the reflectivity $R(\lambda)$ for wavelength λ and the thickness of ink d is given as:

$$R(d, \lambda) = e^{-2K(\lambda)d} R_g(\lambda), \quad (1)$$

where $K(\lambda)$, and $R_g(\lambda)$ are absorption coefficient and reflectivity of the background for λ , respectively. In the case of a scanner image, the color C_i of the i -th channel for a pixel with spectral distribution function $E(\lambda)$ and sensitivity function $q_i(\lambda)$ of the i -th sensor can be given as:

$$C_i(d) = \int_{\Omega_i} R(d, \lambda) q_i(\lambda) E(\lambda) d\lambda, \quad (i=1,2,3) \quad (2)$$

where Ω_i is the wavelength region for the i -th channel. As a rough approximation, if $R(d, \lambda)$ in Ω_i is almost constant and $K(\lambda) \sim K_i$, then (2) can be rewritten as follows.

$$C_i(d) \approx e^{-2K_i d} \int_{\Omega_i} R_g(\lambda) q_i(\lambda) E(\lambda) d\lambda = e^{-2K_i d} C_i^B \quad (3)$$

In (3), $\mathbf{C}^B = (C_1^B, C_2^B, C_3^B)$ denotes the background color (BGC). The SMM cannot explain the brightness reversal of the back- and foreground shown in the example in Fig. 4 b.



a. Original image b. $\gamma=5$ transformed image

Figure 4. Color distribution of gel ink images

B. Kubelka-Munk Models

Kubelka-Munk model (KMM) [11] is a well-known for introducing the effects of light scattering and absorption to solve the brightness reversal problem. Numerous extended KMMs have also been proposed, including the 4-flux model [12] that introduced the effect of reflection at the air-ink boundary. However, it is nearly impossible to apply these models to the present task because they are extremely complicated and require many parameters.

Fortunately, the degree of reversal is very small as in Fig. 4, and the light scattering coefficient may be sufficiently small compared to the absorption coefficient. Therefore, the mixture is considered to be nearly subtractive.

V. EFFECTIVE MODEL OF COLOR-MIXING

A. Proposal of a New Effective Model

The ideal model should satisfy the following conditions:

- The postprint color approaches a dark point \mathbf{T} that is independent of the BGC, as d approaches infinity.
- The color is a function of thickness d of the ink and its output is equal to the center \mathbf{C}^B of the BGC at $d=0$.

- The pixel color $C(d)$ and C^B are smoothly connected because of the Gaussian blurring at the boundary.
- Even when C^B is equal to $\mathbf{0}$, $C(d)$ is not $\mathbf{0}$.

In considering these conditions, we propose a subtractive model of the “n=1 Yule-Nielsen” [11] type as (4).

$$C_i(d) = T_i + e^{-2K_i d} (C_i^B - T_i) \quad (i=1,2,3). \quad (4)$$

The model satisfies the following boundary conditions:

$$\lim_{d \rightarrow 0} C_i(d) = C_i^B, \quad \lim_{d \rightarrow \infty} C_i(d) = T_i.$$

B. Color-Mixing Correction Using the Model

If the proposed model is approximately valid, the postprint color on any background color can be transformed to that on white. According to (4), the color functions for an ink $C^0(d)$, $C^1(d)$ on two different BGCs C^{B0} , C^{B1} are,

$$\begin{aligned} C_i^0(d) &= T_i + e^{-2K_i d} (C^{B0}_i - T_i), \\ C_i^1(d) &= T_i + e^{-2K_i d} (C^{B1}_i - T_i). \end{aligned} \quad (5)$$

Rearranging (5), the following relation can be obtained:

$$\begin{aligned} C_i^1(d) &= T_i + (C_i^0(d) - T_i) \frac{(C^{B1}_i - T_i)}{(C^{B0}_i - T_i)} \quad \text{for } C^{B0}_i \neq T_i, \\ C_i^1(d) &= C^{B0}_i \quad \text{otherwise.} \end{aligned} \quad (6)$$

The observed color of the postprint can be transformed by using (6). In real calculations, $C^{B0}_i \gg T_i$ should be satisfied.

C. Estimation Method of Model Parameters

First, the following space curve formula (7) is obtained by elimination of d from (5).

$$\begin{aligned} \left(\frac{C_1 - T_1}{C^{B1}_1 - T_1} \right)^{\frac{1}{\alpha}} &= \left(\frac{C_2 - T_2}{C^{B2}_2 - T_2} \right)^{\frac{1}{\beta}} = \left(\frac{C_3 - T_3}{C^{B3}_3 - T_3} \right), \\ \alpha &= K_1 / K_3, \quad \beta = K_2 / K_3, \quad C^{B_i} > T_i. \end{aligned} \quad (7)$$

The colors of the pixels are assumed to distribute along (7).

To calculate the parameters $\{\mathbf{T}, \alpha, \beta\}$, 2 sets of images with different background colors $\{C^{B0}, C^{B1}\}$ and the same ink are required. C^{B0} is regarded as a base BGC, for which normally chosen color is white. Fig. 5 shows the idea underlying the calculation. Each approximation curve of the distribution is assumed to start from its BGC and cross \mathbf{T} . The coordinates for \mathbf{T} are expected to take values that are so small that they cannot be estimated correctly. Therefore, we let $T_1=T_2=T_3=T$ for simplicity. We transform the variables as,

$$X_i = \log(C_i - T), \quad X^B_i = \log(C^B_i - T), \quad (8)$$

Equation (8) can be changed to the linear equations,

$$\begin{aligned} X_1 &= X^B_1 + \alpha(X_3 - X^B_3), \\ X_2 &= X^B_2 + \beta(X_3 - X^B_3). \end{aligned} \quad (9)$$

The curve-fitting can be reduced to line-fitting by the linear least-squares method (LLS).

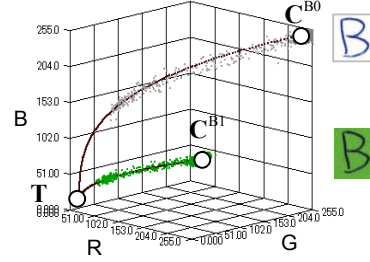


Figure 5. Parameter calculation: approximation curves are added to the figure

We calculate the parameter set using the recursive LLS, according to the following steps:

Step 1: Binarize two learning images I_0 and I_1 . Choose white BGC for I_0 and another BC for I_1 . Average BGCs used for approximate values of C^{B0} and C^{B1} should satisfy the conditions below in (10).

$$\begin{aligned} (\overline{C^{B0}_i} - \overline{C^{B1}_i}) &\geq 2\sigma, \quad (i=1,2,3) \\ \cos^{-1} \left(\frac{\overline{C^{B0}} \cdot \overline{C^{B1}}}{|\overline{C^{B0}}| |\overline{C^{B1}}|} \right) &> \theta_{th}. \end{aligned} \quad (10)$$

where σ is the standard deviation of the base BGC and θ_{th} is a threshold angle between BGC vectors.

Step 2: Set the initial value of T .

Step 3: Calculate (α, β) for T using the LLS. Squared errors for each foreground pixel are calculated as,

$$\begin{aligned} E &= \frac{1}{2} \sum_{m=0}^1 \frac{1}{N_m} E_m, \\ E_m &= \sum_{k=1}^{N_m} \sum_{i=1}^2 \{X^k_i - X^{Bm}_i - w_i(X^k_3 - X^{Bm}_3)\}^2, \end{aligned} \quad (11)$$

where $(w_1, w_2) = (\alpha, \beta)$ and N_m is the number of foreground pixels of image I_m .

Step 4: Increase $T = T + \delta T$.

Step 5: Recursively execute steps 3 and 4 until E reaches the minimum value and determine $\{\mathbf{T}, \alpha, \beta\}$.

VI. COPYRIGHT FORMS AND REPRINT ORDERS

A. Calculation of Parameters

Seven, three, and four colors for the paper, oil ballpoint pens, and gel ballpoint pens, respectively are used to obtain

the experimental data. Characters are written on each paper with a particular pen, and the papers are scanned at 200 dpi by a flathead scanner. The θ_h is set to 12° . Representative colors of the observed backgrounds are shown in Table I. The names for the ink and background colors are inexact. They are adopted from a catalogue for labeling purposes.

TABLE I. BACKGROUND COLORS

| | White | YellowGreen | Cream | Pink | Gray | PaleBlue | DarkLilac |
|---|-------|-------------|-------|-------|-------|----------|-----------|
| R | 247.4 | 99.3 | 247.4 | 230.8 | 91 | 85.5 | 115.1 |
| G | 247.7 | 175.5 | 247 | 87.6 | 103.4 | 163.4 | 104.4 |
| B | 245.9 | 60.1 | 123.4 | 136.9 | 105.5 | 225.6 | 150.2 |

The calculated results of the parameters are indicated in Tables I and II. They are average values obtained from up to 6 pairs of images. Curve-fitting results for oil inks using the parameter set calculated by the white and yellow-green BGC pair are shown in Fig. 6 as an example. Each curve is drawn according to (7) by entering its representative BGC. All curves for an ink are drawn in a same $/RGB$ space.

TABLE II. ESTIMATION RESULT: OIL INK

| | Black | Blue | Red |
|----------|-------------------|-------------------|-------------------|
| α | 1.099 ± 0.001 | 3.655 ± 0.002 | 0.092 ± 0.001 |
| β | 1.119 ± 0.002 | 3.329 ± 0.034 | 1.056 ± 0.001 |
| T | 21.28 ± 0.64 | 19.20 ± 1.73 | 21.60 ± 0.01 |

TABLE III. ESTIMATION RESULT: GEL INK

| | Black | Blue | Red | Green |
|----------|-------------------|-------------------|-------------------|-------------------|
| α | 1.028 ± 0.004 | 2.454 ± 0.014 | 0.010 ± 0.001 | 1.593 ± 0.030 |
| β | 0.974 ± 0.003 | 2.237 ± 0.085 | 1.031 ± 0.003 | 0.715 ± 0.003 |
| T | 16.48 ± 2.89 | 15.68 ± 2.33 | 19.00 ± 4.50 | 9.60 ± 2.53 |

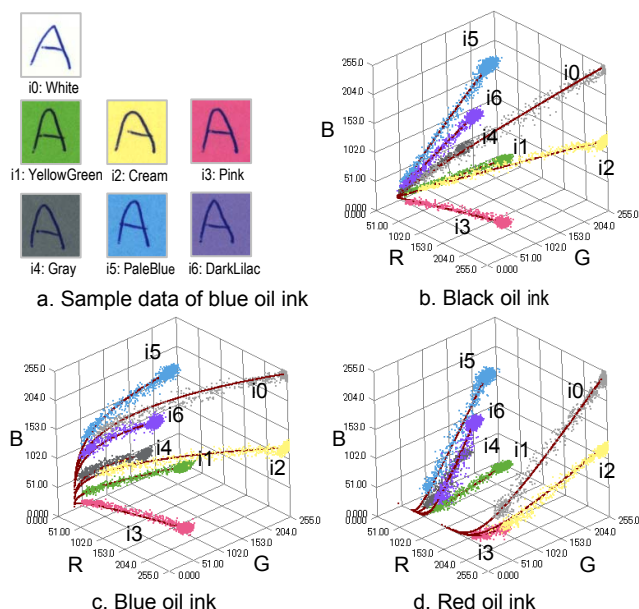


Figure 6. Curve-fitting results for oil inks using white and yellow-green BGC Images

From these results, it is observed that the $n=1$ Yule-Nielsen-type model with Beer-Lambert's law applies well to postprints by oil and gel inks in scanner images.

B. Comparizon to Line Approximation

A comparison is made between the line-fitting model and the proposed model by the squared errors from the approximated line/curve. The least-squares method is used for the line approximation. White background images are used for this experiment because the curvatures are often hidden in the heat noise in the case of other BGCs with larger absorption values. The results are shown in Tables IV and V, and examples of the fitting results using the proposed model and the line-fitting model are shown in Fig. 7. The three curve-fitting cases in the tables below correspond to the average errors calculated by all possible image pairs, the best image pairs, and the worst image pairs, respectively.

TABLE IV. SQUARED ERRORS: OIL INK

| | Black | Blue | Red |
|---------------|-------|-------|-------|
| Line | 111.4 | 134.3 | 105.7 |
| Curve (avr.) | 114.3 | 74.7 | 98.7 |
| Curve (best) | 114.1 | 61.0 | 98.7 |
| Curve (worst) | 114.3 | 98.1 | 98.7 |

TABLE V. SQUARED ERRORS: GEL INK

| | Black | Blue | Red | Green |
|---------------|-------|-------|-------|-------|
| Line | 174.5 | 377.6 | 134.1 | 337.3 |
| Curve (avr.) | 170.7 | 209.1 | 132.7 | 186.4 |
| Curve (best) | 170.0 | 204.6 | 131.8 | 181.1 |
| Curve (worst) | 171.3 | 219.0 | 133.0 | 196.4 |

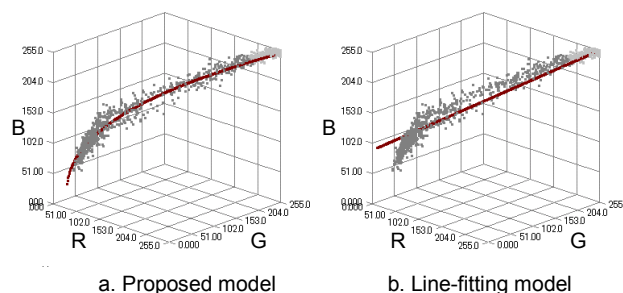


Figure 7. Fitting results: Blue gel ink

From Tables IV and V, the errors for the blue and green inks by the proposed model are clearly smaller than those by the line-fitting model. On the other hand, the errors for the black and red inks are almost identical between the two methods. This is because the colors of black and red inks distribute almost along a line to which both models are applicable. In the former case, absorption levels of the RGB channels are thought to be almost equal. In the latter case, the absorption level is thought to be very small for the R channel compared to the other channels. Therefore, the colors of each BGC distribute almost along a line on the G-B plane.

C. Color-Mixing Correction

In this section, experiments were performed on color-mixing correction. An image with a non-white BGC is converted into that with a white BGC by (6), and the accuracy is evaluated by Kullback-Leibler (KL) divergence and distance between the average foreground color (D) and its true color (white BGC image). T is set to 20.

TABLE VI. RESULTS FOR MIXING CORRECTION

| Ink color | Before | | After | |
|-----------|--------|------|-------|------|
| | KL | D | KL | D |
| Black oil | 9.73 | 51.7 | 0.45 | 7.4 |
| Blue oil | 9.57 | 65.7 | 0.51 | 11.1 |
| Red oil | 9.38 | 67.7 | 0.40 | 9.9 |
| Black gel | 9.25 | 41.2 | 0.43 | 12.1 |
| Blue gel | 9.35 | 46.5 | 0.46 | 6.8 |
| Red gel | 9.41 | 62.1 | 0.45 | 13.5 |
| Green gel | 9.36 | 48.2 | 0.51 | 6.8 |

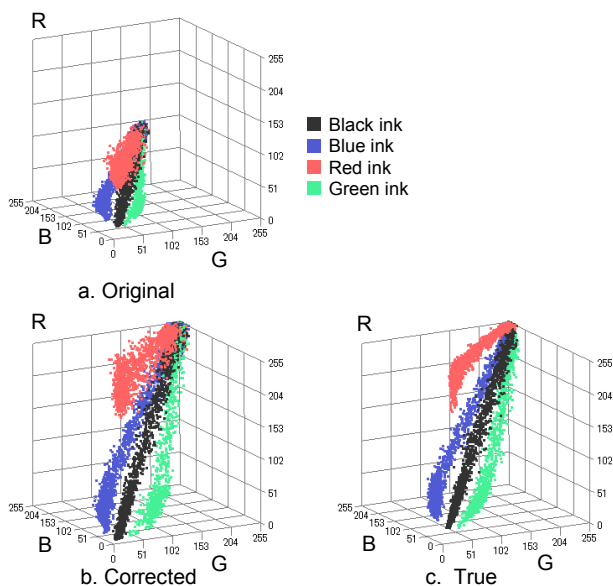


Figure 8. Example: Distribution of colors of gel inks on pale-blue

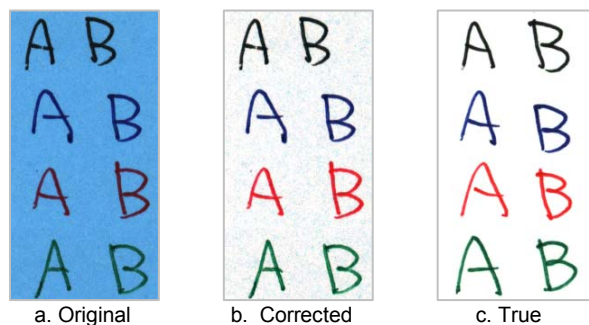


Figure 9. Example: Images of gel inks on pale-blue

The results indicated in Table VI show that with the proposed method, the color distribution of the postprint on a colored background is close to that on a white background. Fig. 8 depicts an example of the distributions before and after the correction for 4 ink colors on pale blue. The actual images are shown in Fig. 9.

VII. CONCLUSIONS AND REMARKS

An effective color-mixing model is constructed for scanner images with postprints and a method to correct the mixing of colors is proposed. The model parameters of the model were determined by a pair of images with different BGCs. The experimental results confirm the effectiveness of the approach.

The limits of this method are thought to be the following:

- Non-opaque ink with non-negligible scattering coefficients
- Paper of too dark a color
- Nonreciprocal compressed image such as a JPEG
- Inks with highly different properties existing together in a target field

The fourth item is familiar for handwritten forms, where preprints and postprints are used together. In the future, it will be necessary to construct functions to distinguish both patterns and execute different processing for each component.

ACKNOWLEDGMENT

The author would like to thank Dr. Ohta, Mr. Takebe, Dr. Zheng, Mr. Inami, Mr. Shimazaki, and other coworkers for their valuable comments and supports. Especially, this paper could not be accomplished without Mr. Shimizu's advice.

REFERENCES

- [1] N. Ohta, Reflection Density of Multilayer Color Prints I. Specular Reflection Density, *Phot. Sci. Eng.* **Vol.15**, No.6, 1971, pp.487-494.
- [2] A. Murray, Monochrome Reproduction in Photoengraving, *J. Franklin Institute*, **Vol.221**, 1936, pp.721-724.
- [3] T. Porter and T. Duff, Compositing Digital Images, *Computer Graphics*, **Vol.18**, No.3, 1984, pp.253-259.
- [4] T. Terai *et al.*, The Base Color Recognition by Tetragonal Regression for Overlapped Watercolors, *IWFHR*, 2004, pp.551-556.
- [5] M. Worring *et al.*, Segmentation of Color Documents by Line Oriented Clustering Using Spatial Information, *ICDAR*, 99, pp.67-70.
- [6] Y. He, Unsupervised Decomposition of Color Document Images by Projecting Colors to a Spherical Surface, *DAS*, pp.394-401, 2008.
- [7] D. Zheng *et al.*, Separation of Overlapped Color Planes for Document Images, *ICIP*, 2010, pp.1949-1952.
- [8] M. Suwa and K. Fujimoto, Color Mixing Correction for Postprinted Patterns on Colored Background Using Modified Particle Density Model, *IWFHR*, 2006, pp.557-562.
- [9] J. Yule and W. Nielsen, The Penetration of Light into Paper and Its Effect on Halftone Reproduction, *TAGA*, 1951, pp.65-76.
- [10] A. Beer, Bestimmung der Absorption des rothen Lichts in farbigen Flüssigkeiten, *Ann. Physik*, **Vol.162**, 1852, pp.78-88.
- [11] V. P. Kubelka and F. Munk, Ein Beitrag zur Optik der Farbanstriche, *Zeits. fur Techn. Physik*, **Vol. 12**, 1931, pp.593-601.
- [12] W. E. Vargas and G. A. Niklasson, Applicability conditions of the Kubelka-Munk theory, *Appl. Opt.* **Vol. 36**, 1997, pp.5580-5586.